Psychiatry Research: Neuroimaging 320 (2022) 111441

Contents lists available at ScienceDirect

Psychiatry Research: Neuroimaging

journal homepage: www.elsevier.com/locate/psychresns

Functional reconfiguration of cerebellum-cerebral neural loop in schizophrenia following electroconvulsive therapy

Hao Hu [a,1], Yuchao Jiang [b,1], Mengqing Xia [a], Yingying Tang [a], Tianhong Zhang [a], Huiru Cui [a], Junjie Wang [c], Lihua Xu [a], Adrian Curtin [d,e], Jianhua Sheng [a], Xinyi Cao [a], Qian Guo [a], Yuping Jia [a], Chunbo Li [a,f,g], Zhen Wang [a,*], Cheng Luo [b,*], Jijun Wang [a,f,g,**]

[a] Shanghai Key Laboratory of Psychotic Disorders, Shanghai Mental Health Center, Shanghai Jiao tong University School of Medicine, Shanghai 200030, China
[b] Key Laboratory for NeuroInformation of Ministry of Education, School of Life Science and Technology, University of Electronic Science and Technology of China, Chengdu 610054, China
[c] Institute of Mental Health, Suzhou Psychiatric Hospital, The Affiliated Guangji Hospital of Soochow University, Suzhou, Jiangsu, 215137, China
[d] School of Biomedical Engineering & Health Sciences, Drexel University, Philadelphia, PA 19104, United States
[e] Med-X Institute, Shanghai Jiao Tong University, Shanghai 200300, China
[f] CAS Center for Excellence in Brain Science and Intelligence Technology (CEBSIT), Chinese Academy of Science, Shanghai, China
[g] Institute of Psychology and Behavioral Science, Shanghai Jiao Tong University, Shanghai, China

ARTICLE INFO

Keywords:
Schizophrenia
ECT
Cerebellum
Large scale network

ABSTRACT

Recent evidence highlights the role of the cerebellum-cerebral loop in the pathophysiology of schizophrenia (SZ). Electroconvulsive therapy (ECT) is clinically applied to augment the effect of antipsychotic drugs. The study aims to address whether the cerebellum-cerebral loop is involved in the mechanisms of ECT's augmentation effect. Forty-two SZ patients and 23 healthy controls (HC) were recruited and scanned using resting-state functional MRI (rs-fMRI). Twenty-one patients received modified ECT plus antipsychotics (MSZ group), and 21 patients took antipsychotics only (DSZ group). All patients were re-scanned four weeks later. Brain functional network was constructed according to the graph theory. The sub-network exhibited longitudinal changes after ECT or medications were constructed. For the MSZ group, a sub-network involving default-mode network and cerebellum showed significant longitudinal changes. For the DSZ group, a different sub-network involving the thalamus, frontal and occipital cortex was found to be altered in the follow-up scan. In addition, the changing FC of the left cerebellar crus2 region was correlated with the changing scores of the psychotic symptoms only in the MSZ group but not in the DSZ group. In conclusion, the cerebral-cerebellum loop is possibly involved in the antipsychotic mechanisms of ECT for schizophrenia.

1. Introduction

Nearly 30% of schizophrenia (SZ) patients, who constitute a significant proportion of chronic schizophrenia, do not respond well to antipsychotics, especially those who exhibited sustained positive symptoms (Meltzer, 1997). Recent evidence shows that SZ with negative symptoms and cognitive deficits also responds poorly to antipsychotics (Elkis, 2007, Howes et al., 2017). In clinical practice, electroconvulsive therapy (ECT) has been applied to augment antipsychotic effects, especially for treatment-resistant SZ (Tharyan and Adams, 2005, Lally et al., 2016). However, the underpinning mechanisms of antipsychotic effects of ECT remain largely unknown. Although the mechanisms have been explored in several domains, including dopamine serotonin neurotransmitter activity, neurotrophic effects, immune system modulation, and functional disconnections (Jiang et al., 2017), no consensus has been achieved.

Recently, the role of the cerebellum in the pathophysiology of SZ has attracted attentions from researchers. The cerebellum is highly

* Corresponding authors.
** Corresponding author at: Shanghai Key Laboratory of Psychotic Disorders, Shanghai Mental Health Center, Shanghai Jiao Tong University School of Medicine, Shanghai 200030, China.
E-mail addresses: wangzhen@smhc.org.cn (Z. Wang), chengluo@uestc.edu.cn (C. Luo), jijunwang27@163.com (J. Wang).
[1] These authors contributed equally to this work.

https://doi.org/10.1016/j.pscychresns.2022.111441
Received 28 April 2021; Received in revised form 15 November 2021; Accepted 17 January 2022
Available online 22 January 2022

developed in humans and proved to be involved in several essential higher-order processes. Recent studies show that the cerebellum is involved in the process of emotion (Flace et al., 2018), cognition (Sokolov et al., 2017, Wang et al., 2019, Castellazzi et al., 2018), or even social behaviors (Carta et al., 2019), and suggest the cerebellum as one key candidate for the prevalence of psychiatry disease (Villanueva, 2012, Andreasen and Pierson, 2008, Hirjak et al., 2015, Sathyanesan et al., 2019, Chen et al., 2019). Evidence shows that the cerebellum-cortical neural loop might be involved in the mechanism of both negative and positive symptoms of schizophrenia. For example, decreased functional activity in the cerebellum in SZ is observed during the emotional task (Surguladze et al., 2011). Negative symptoms significantly correlated with functional connectivity (FC) between the cerebellum and prefrontal cortex, and the abnormality could be restored by transcranial magnetic stimulation (TMS) targeting the cerebellum midline (Brady et al., 2019). The FC between right-hemispheric VI in the cerebellum and right fusiform cortex was decreased in SZ and correlated with positive symptoms (Zhuo et al., 2018). The involvement of the cerebellum in the mechanism of SZ is further supported by one recent research, which indicated that impaired FC of cerebellum with cerebrum could be restored by antipsychotics (Guo et al., 2018), providing one potential mechanism of antipsychotics' SZ. In the present study, we proposed that the cerebellum played a crucial role in the antipsychotic mechanisms of ECT.

Evidence shows that ECT relieves psychotic symptoms. The negative symptom has long been considered drug-resistant yet can be significantly reduced by ECT (Pawelczyk et al., 2014). ECT is also reported to improve both positive and negative symptoms, as reported by one naturalistic observational study (Usta Saglam et al., 2020). Considering cognition impairment, ECT is mainly applied in treatment-resistant SZ as an augmentation on antipsychotics, which limits the number of researches focusing on the efficacy mechanism of ECT on SZ. However, one recent research shed light on the awkward situation. Thomann and colleagues conducted a longitudinal study focusing on the different mechanisms regarding the efficacy effects of ECT on SZ and major depression disorder (MDD). They found that there is a transdiagnostic effect of ECT on FC regardless of diagnosis (Thomann et al., 2017). The seizure induced by ECT is thought to alter functions of the whole brain, including the cerebellum. Previous research indicated that the regional blood flow in the cerebellum was increased following ECT, suggesting ECT might alter the functional state of the cerebellum (Takano et al., 2011). One ECT research revealed that cerebellum-cerebral FC alternations might be contributed to the mechanism of ECT efficacy on MDD (Wei et al., 2020). Given the evidence mentioned above, cerebellum-cerebrum FC may also be involved in the mechanism of ECT efficacy on SZ.

The current study investigated the mechanism of ECT's efficacy on SZ via resting-state MRI. We hypothesized ECT would improve positive symptoms and negative symptoms by mainly acting on FC between the cerebellum and cerebrum. More specifically, some features of the cerebellum-cortical neural loop might change in response to ECT.

2. Methods

2.1. Participants

Forty-two acute SZ patients were allocated into two groups under the psychiatrists' strategy. Twenty-one patients received a 4-week course of modified ECT treatment plus antipsychotics (MSZ group). Meanwhile, the other 21 patients only received antipsychotic drugs for 4-weeks (DSZ group).

SZ patients were recruited from the inpatient department of Shanghai Mental Health centre (SMHC). Senior psychiatrists made these patients' diagnoses with SCID-I/P (Structural Clinical Interview for DSM-IV-TR, Patient edition). All patients were not treated with ECT within the previous six months. The symptoms' severity was assessed with the Positive and Negative Syndrome Scale (PANSS). The baseline clinical assessments were conducted within two days after the patients signed the consent forms. For the MSZ group, their clinical assessment must be finished before the first session of ECT. The baseline PANSS total score of included subjects had to be higher than sixty. The antipsychotic dosage was measured by chlorpromazine equivalents (mg/d) according to the conversion protocol as proposed by Andreasen and his colleagues (Andreasen et al., 2010). For the MSZ group, we did the follow-up clinical assessment two days after the final session of ECT. For the DSZ group, their follow-up clinical assessment would be conducted four weeks after their initial assessment. Exclusion criteria were brain injuries; history of neurological illness; severe physical diseases; dementia; substance abuse or dependence within six months; contraindications to MRI. The dosages of antipsychotic drugs were constant during the whole study phase.

Twenty-three healthy controls were recruited in parallel, with age and sex-matched with the patients' group. Exclusion criteria included a history of current or past diagnosis of mental disorders; positive family history of psychosis; brain injuries; history of neurological illness; severe physical illnesses; dementia; substance abuse or dependence within six months; contraindications to MRI. The study protocol was approved by Ethnic Committee in Shanghai Mental Health Center. Written informed consent for participation was obtained from each subject and their family. All study procedures were under the Declaration of Helsinki, version 1989.

2.2. Modified electroconvulsive therapy

Patients in the MSZ group would finish clinical assessment before ECT therapy. Acute ECT protocol was administered to all the patients in the MSZ group, while no patients received maintenance ECT protocol. ECT was administered every other day during workdays. ECT was administrated by bilateral electrical stimulation with a Thymatron System IV (Somatics, Lake Bluff, IL, USA). Anesthesia was induced by intravenous etomidate (0.21–0.3 mg/kg) in combination with propofol (1.82–2.44 mg/kg) to keep patients from discomforts related to convulsion. Intravenous succinylcholine (1 mg/kg) was used to reduce the risk of bone fracture. Intravenous atropine (0.5 mg) was applied to inhibit airway secretion. The dosage of antipsychotics in the MSZ group wasn't altered until the termination of ECT therapy. Bitemporal stimulus is widely used in clinical practice and has the advantage of fast clinical remission, although at the cost of short-term memory impairments (C.H. Kellner et al., 2010, C.H. Kellner et al., 2010). Stimulus electrodes were placed on the bitemporal scalp to induce convulsion, monitored by electroencephalogram, with ECT parameters: maximum charge delivered, 504mC; output current, 0.9 A; frequency, 10–70 Hz; pulse width, 1.0 ms; maximum stimulus duration, 8 s. The duration of the current induced seizure, as recorded by electroencephalogram, lasted between 25 s and 60 s. Thymatron System IV can offer stimulus train up to 8 s at maximum, available for more pulses, and reduce cognitive side effects (Peterchev et al., 2010). Patients in our study received at least eight times of ECT therapy (1 MSZ, 8 times; 3 MSZs, 10 times; 1 MSZ, 11 times; 16 MSZs, 12 times). The number of ECT sessions was determined by a senior psychiatrist mainly according to the patients' efficacy and tolerance. If subjects had a good response to ECT even with fewer than eight sessions, at least 8 ECT sessions would be prescribed. On the condition of unsatisfied efficacy, the number of ECT sessions could be increased to 12.

2.3. MRI data acquisition

All subjects' MRI data were obtained using a 3.0 T Siemens Magnetom Verio syngo MR B17 scanner. Patients in the MSZ group would be scanned once, 24 h before the first ECT session, and scanned again 24–48 h after the last session of ECT. Patients in the DSZ group would be scanned in parallel for two-time points of the MSZ group. Healthy

controls were scanned once in our study. Subjects were instructed to keep their eyes closed, not focus on anything particularly, and try not to fall asleep.

Resting-state functional MRI data were obtained using a gradient echo planar imaging (EPI) sequence. Thirty slices were acquired with repetition time= 2000 ms; echo time = 30 ms; flip angle = 90°; field of view = 220 mm × 220 mm; matrix = 64 × 64; slice thickness = 4 mm; voxel size=3.4 × 3.4 × 3.4 mm, creating 180 volumes, with a total scanning time of 366 s. T1-weighted images were obtained using a magnetization-prepared rapid acquisition gradient echo (MPRAGE) sequence. Two hundred and twenty-four slices were acquired with TR=2530 ms, TE=2.56 ms, flip angle = 7°, inversion time = 1100 ms, FOV = 256 mm × 256 mm, matrix = 256 × 256, slice thickness = 1 mm, voxel size = 1.0 × 1.0 × 1.0 mm.

2.4. fMRI data preprocessing

Functional data preprocessing was similar to our prior studies (Jiang et al., 2019, Huang et al., 2018), including removal of the first ten TRs, slice-timing, realignment, normalization, linear detrending, nuisance signals regression, filtering (0.01–0.1 Hz), and smoothing (full width at half maximum=6 mm). All subjects weren't excluded based on head motion measured with the MRI scans' framewise displacement (FD).

2.5. fMRI network construction and graph analysis

We used GRaph thEoreTical Network Analysis (GRETNA, http://www.nitrc.org/projects/gretna/) to construct and analyze the brain fMRI network (Wang et al., 2015). GRETNA is used for brain connectomics analysis. The GRETNA is an open-source, Matlab-based, cross-platform (Windows and UNIX OS) package with a graphical user interface (GUI). It allows topological analyses of global and local network properties. The GRETNA has been used for brain network analysis in many brain disorders such as SZ, depression, and autism (Guo et al., 2019, Jiang et al., 2020). Firstly, the Automated Anatomic Labeling atlas (AAL) was employed to parcellate the brain into 116 regions of interest (ROIs) (90 in cerebrum and 26 in cerebellum), which was introduced in 2002 (Tzourio-Mazoyer et al., 2002). The AAL ROIs were defined as the nodes for the fMRI network. Subsequently, the averaged time series of all voxels in each ROI were computed; the Pearson's correlational coefficients between the mean time series of all pairs of ROIs were used to measure the functional connectivity (FC) among regions. The FC was used to define the edges of the fMRI network. This yielded a 116 × 116 FC matrix for each subject. Finally, each FC matrix was further transformed into an undirected binarized matrix using a sparsity threshold. According to previous research (Yu et al., 2017), we chose a wide range of sparsity (8% to 50% with an interval of 0.01) to threshold the FC matrix. This thresholding yielded a set of 116 × 116 binarized matrices for each subject.

To characterize the topological properties of brain networks, we calculated the network measures including global efficiency (E_{glob}), local efficiency (E_{loc}), clustering coefficient (C_p), and small-worldness metric (σ) for the brain network at each sparsity threshold. In terms of graph theory, the E_{glob} of a network represents the ability of parallel information transmission over the network. The E_{loc} measures the averaged local efficiencies of all the network nodes and indicates the communication speed among the interconnected groups of network nodes. The C_p is defined as the mean clustering coefficients of all the nodes in the network and reveals the degree to which nodes in a network tend to cluster together. The small-worldness σ indicated an optimal balance between high local specialization and high global integration of the brain. Subsequently, we calculated the z-score of topological properties of a network by subtracting the average of each topological property across random networks and dividing it by the standard deviation of random networks. Furthermore, the area under the curve (AUC) for each network metric was calculated to yield a summarized scalar for the topological characterization of brain networks independent of a single threshold selection (Yu et al., 2017, Adhikari et al., 2015). Accumulated evidence has indicated that the AUC is sensitive to detecting network topological alterations in many brain disorders (Yu et al., 2017, Zhang et al., 2011, He et al., 2009).

2.6. Statistical analysis

2.6.1. Comparisons among baseline sz SZ and HC

To investigate the differences of topological organization in the fMRI network between baseline SZ and HC, we combined the MSZ_{t1} group and DSZ_{t1} group into a baseline SZ group. Non-parametric permutation tests were utilized to compare the AUC of each network metric (E_{glob}, E_{loc}, C_p, and σ) between baseline SZ and HC (Adhikari et al., 2015). In brief, we first calculated the between-group difference for each network metric. Then, we randomly assigned the group labels across all subjects and re-calculated the difference between the two randomized groups. This randomization procedure was repeated 100,000 times. The statistical significance was assessed by the 95th percentiles of each null hypothesis distribution, corresponding to a type I error probability of 0.05 for a two-tailed test.

2.6.2. Longitudinal comparisons between pre-treatment and post-treatment

As the sample size was small and the network metrics were not normally distributed, the non-parametric Wilcoxon Signed-rank test was employed to compare the longitudinal changes (t_2 vs. t_1) in each patient group.

2.7. Key sub-network analysis

To further localize the specific brain sub-network in which functional connectivity was altered in response to ECT, we applied the network-based statistics method on the brain regions exhibiting longitudinal changes after treatments (Adhikari et al., 2015). Briefly, three-node centrality metrics, including the nodal degree, efficiency, and betweenness centrality, were calculated for each subject's fMRI network. Then, the non-parametric Wilcoxon Signed-rank test was employed on each node centrality metric to determine significant longitudinal alterations following ECT. Subsequently, the nodes that exhibited significant longitudinal changes in at least one of the nodal centralities were extracted to generate a subset of connection matrices based on these altered nodes. Finally, based on the above connection matrices, the network-based statistics approach was utilized to define one or more sub-networks, which included any connected components exhibiting longitudinal changes after ECT (10,000 permutations, threshold = 2.1, corrected $P<0.05$) (Zalesky et al., 2010). This strategy has been widely used for the detection of abnormal sub-network in brain disorders (Adhikari et al., 2015). Besides, the sub-network analysis was also performed in the DSZ group.

2.8. Associations between key sub-network and symptoms improvements

To investigate the relationship between changes of fMRI network and symptoms improvements, we measured the longitudinal changes ($\triangle=t_2-t_1$) for each FC within key sub-network in the MSZ group. The Spearman rank correlation analysis assessed the associations between $\triangle$FC and reductive ratio of PANSS subscales scores in MSZ. A permutation test procedure was used to control the family-wise error rate (FWE) for multiple comparisons (Groppe et al., 2011).

3. Results

3.1. Demographic and clinical information

Table 1 provides detailed demographic and clinical information for all subjects. There were no significant differences in age, gender, and

Table 1
Demographic data.

	MSZ (n=21)	DSZ (n=21)	HC (n=23)	Statistics
Age (years)	29.2±7.1	30.7±6.9	31.2±5.9	F = 0.494, P = 0.613[a]
Sex(F/M)	11/10	12/9	12/11	χ^2 =0.136, P= 0.934[b]
Education(years)	12.3±3.4	12.6±2.9	13.5±2.5	F = 0.976, P = 0.382[a]
Number of previous failed trials of antipsychotics	3.1±1.1	2.5±1.1	-	t = 1.81, P= 0.077[c]
Chlorpromazine equivalents (mg/d)	604.6±565.6	532.6±461.2	-	t = 0.452, P = 0.653 [c]
Subjects on over 2 antipsychotics (Y/N)	18/3	9/12	-	χ^2 =8.400, P = 0.004[b,*]
Illness duration (months)	79.8±54.4	78.7±80.9	-	t=0.049, P=0.961[c]
Duration of untreated psychosis (months)	19.8±32.1	15.7±34.4	-	t=0.403, P=0.689[c]
Long illness duration (over two years) (Y/N)	18/3	13/8	-	χ2=3.079, P=0.079[b]
Age of first onset	28.2±7.9	28.7±7.8	-	t=-0.643, P=0.524[c]
Baseline PANSS score				
Total	71.6±8.4	70.8±9.7	-	t = 0.425, P = 0.673[c]
Positive	20.7±2.6	19.1±3.5	-	t = 1.651, P = 0.107[c]
Negative	19.3±7.4	17.4±5.1	-	t = 0.967, P = 0.339[c]
General	32.0±3.8	34.2±5.7	-	t =−1.509, P = 0.139[c]
Week-4 PANSS score				
Total	49.7±9.6	50.5±12.6	-	t =−0.234, P = 0.816[c]
Positive	10.9±3.0	12.0±4.7	-	t =−0.897, P = 0.375[c]
Negative	14.6±6.1	14.0±5.3	-	t = 0.297, P = 0.768[c]
General	24.3±3.33	24.5±5.4	-	t =−0.138, P = 0.891

Abbreviation: MSZ, schizophrenia patients allocated to ECT group; DSZ, Schizophrenia patients allocated to drug group; HC, healthy control group; PANSS, positive and negative syndrome scale. *Note*: Number of antipsychotics with no response, failed trials of antipsychotics in patients' previous history.

[*] $P < 0.05$.

[a] Analysis of variance.

[b] Chi-square test

[c] , two-sample *t*-test.

education level among groups (MSZ, DSZ, and HC). The two patient groups showed no differences in terms of the illness duration, duration of current episode, duration of untreated psychosis, age of first onset, antipsychotic dosage represented by chlorpromazine equivalent doses, and the number of failed trials of antipsychotics. The drug information and chlorpromazine equivalents are shown in table 2. There were 2 MSZs and 4 DSZs prescribed with clozapine. The number of SCZ prescribed with clozapine was not significantly different between DSZ and MSZ groups (χ^2=0.194, P=0.659). Twelve DSZs and three MSZs were on single antipsychotics, while nine DSZs and eighteen MSZs were on over two kinds of antipsychotics. The number of patients on single antipsychotic showed statistical significance between DSZ and MSZ group (χ^2=8.400, P=0.004). The proportion of patients with a long duration of illness (over two years) in the MSZ group was marginally higher than the proportion in the DSZ group (χ2=3.079, P=0.079).

3.2. Global topological organization of fMRI network

The fMRI network analysis showed that: (1) at baseline, the patients with SZ showed higher E_{glob} (P=0.0121, FWE corrected) and trends toward lower E_{loc} (P=0.0669, FWE corrected) compared with the HC; (2) after the ECT treatment, the MSZ_{t2} group exhibited reduced E_{glob} (P=0.0325, FWE corrected) and increased E_{loc} (P=0.0355, FWE corrected) of the fMRI network than the MSZ_{t1} group; (3) there was no significant change of E_{glob} or E_{loc} between the DSZ_{t1} and DSZ_{t2} groups (all Ps>0.05) (Fig. 1).

3.3. Key fMRI sub-network with altered FC following ECT

Baseline comparisons showed ten brain regions exhibited significance in at least one nodal metric between SZ and HC (Table 3). These regions were mainly located in the occipital lobe, temporal lobe, and cerebellum (Fig. 2A). Using network-based statistics, we identified a sub-network with five nodes and three connections that were significantly altered in the SZ group (P<0.05, FWE corrected) (Fig. 2B). Specifically, the 3 FCs within the sub-network were reduced in the SZ group, compared with the HC group.

After ECT, significantly longitudinal changes were observed in 22 brain regions, mainly located in the frontal lobe and cerebellum (Fig. 2C, Table 4). Further network-based statistics analysis showed a connected sub-network with 17 nodes and 40 connections that were significantly altered following ECT (P<0.05, FWE corrected) (Fig. 2D). The ECT key sub-network nodes included several default-mode network (DMN) regions and cerebellar regions. The key sub-network connectivity was primarily involved in the connections that link the DMN and the cerebellum. Within this sub-network, the connections exhibited significantly increased values in the patients following ECT.

As for the DSZ group, we identified 18 brain regions that exhibited significant longitudinal changes (Table 5). These regions were mainly located in the frontal lobe, occipital lobe, and cerebellum (Fig. 2E). The network-based statistics analysis showed a connected sub-network with 13 nodes and 13 connections that were significantly altered following antipsychotic treatment in the DSZ group (P<0.05, FWE corrected) (Fig. 2F). The key sub-network nodes included cerebral cortical regions, thalamus, and cerebellar regions. The key sub-network connectivity was primarily involved in the connections that link the thalamus and the cerebral cortices. Within this sub-network, the connections exhibited significantly increased values in the patients following antipsychotic treatment.

3.4. Associations between key sub-network FC and symptoms improvements

The ECT-induced △FC between the left middle temporal gyrus and left cerebellar crus2 region showed significant correlations with the reductive ratio of the PANSS total scores (R=0.438, P=0.047, uncorrected, Fig. 3A) and the reductive ratio of the PANSS general psychopathology subscales (R=0.580, P=0.006, FWE corrected, Fig. 3B) in the MSZ group. In addition, the △FC between the left inferior temporal gyrus and left cerebellar crus2 region exhibited a significant correlation with the reductive ratio of the PANSS general psychopathology subscales (R=0.610, P=0.003, FWE corrected, Fig. 3C) in the MSZ group. The △FC between right angular and left cerebellar 45 regions were significantly correlated with the reductive ratio of the PANSS general psychopathology subscales (R=0.467, P=0.033, uncorrected, Fig. 3D) in the MSZ group. There were no such correlations in the DSZ group.

4. Discussion

Our present study was the first to investigate the changes of the cerebellum-cerebrum circuit in response to ECT in patients with SZ. Our study has several significant findings: (1) SZ group exhibited abnormal

Table 2
Antipsychotics prescribed to SZ patients.

DSZ Drug	Subject number	Average chlorpromazine equivalents	MSZ Drug	Subject number	Average chlorpromazine equivalents
Olanzapine Amisulpride Paliperidone ER	1	845.5	Risperidone Olanzapine	3	425
Olanzapine Risperidone	1	250	Quetiapine Paliperidone ER	1	250
Ziprasidone Olanzapine	1	366.7	Amisulpride Aripiprazole Clozapine	1	2256.8
Clozapine Risperidone	2	475	Clozapine Aripiprazole	1	316.7
Olanzapine Paliperidone ER	1	325	Paliperidone ER Haloperidol Quetiapine	1	800
Penfluridol Quetiapine	1	1266.7	Risperidone Quetiapine	1	283.3
Paliperidone ER Aripiprazole	1	108.3	Risperidone Paliperidone ER	1	162.5
Amisulpride Aripiprazole	1	1024.2	Paliperidone ER Clozapine Amisulpride	1	891
Risperidone	6	195.8	Olanzapine Haloperidol	1	650
Amisulpride	2	1436.3	Olanzapine Perphenazine	1	480
Olanzapine	1	400	Chlorpromazine Paliperidone ER	1	325
Aripiprazole	1	200	Ziprasidone Olanzapine	1	283.4
Ziprasidone	1	200	Ziprasidone Quetiapine Amisulpride	1	1682.3
Quetiapine	1	1200	Olanzapine Ziprasidone Clozapine	1	616.7
			Olanzapine Amisulpride Risperidone	1	1549
			Risperidone	2	175
			Olanzapine Paliperidone ER	1	337.5
			Paliperidone ER	1	187.5

Abbreviation: SZ, schizophrenia; DSZ, schizophrenia patients allocated to drug group; MSZ, schizophrenia patients allocated to ECT group; ER, extended-release.

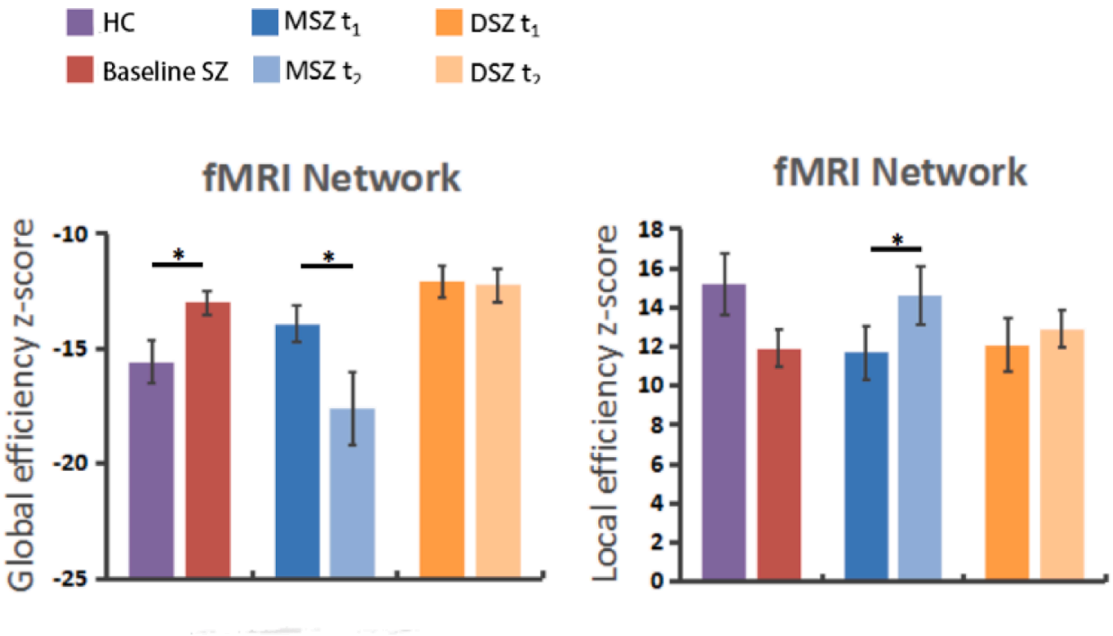

Fig. 1. The bar graph shows the network topological metrics of E_{glob} and E_{loc} among the HC, Baseline HC, MSZ_{t1}, MSZ_{t2}, DSZ_{t1}, and DSZ_{t2}. SZ, schizophrenia; MSZt1, schizophrenia patients at pre-ECT; MSZt2, schizophrenia patients at post-ECT; DSZt1, schizophrenia patients pre-antipsychotics; DSZt2, schizophrenia patients at post-antipsychotics.

global efficiency and local efficiency, which could be improved by ECT. (2) Cerebellum was involved in the mechanism of the efficacy effect of both antipsychotic and ECT. (3) ECT-induced changes of FC correlated with clinical improvements.

For the baseline fMRI network analysis, our research revealed higher global efficiency and lower local efficiency in SZ patients, which was in line with previous studies (Alexander-Bloch et al., 2010, Lynall et al., 2010, Micheloyannis, 2012). We believe that these abnormalities indicate the efficient information processing may be at the cost of lowering the local fault tolerance, which might account for the generation of delusion in SZ, as proposed by the hypothesis of jumping to the conclusion (Moritz and Woodward, 2005). Some fMRI researches also reported the opposite results, which showed lower global efficiency or increased local efficiency in schizophrenia (Ganella et al., 2017, Sun et al., 2019, Su et al., 2015). The conflicting results may come from differences in methodology, race, or illness state. For the methodology

Table 3
Brain regions exhibited significant between-group differences in at least one nodal metric in patients with schizophrenia versus healthy controls.

Regions	AAL Labels	Abbreviation	Permutation test p-values		
			Efficiency	Betweenness	Degree
Right middle frontal cortex	Frontal_Mid_R	MFG.R	0.028*	0.029*	0.015*
Right inferior occipital cortex**	Occipital_Inf_R	IOG.R	0.011*	0.019*	0.028*
Right fusiform	Fusiform_R	FFG.R	0.025*	0.091	0.061
Right paracentral lobule	Paracentral_Lobule_R	PCL.R	0.030*	0.022*	0.372
Left caudate**	Caudate_L	CAU.L	0.100	0.015*	0.146
Right thalamus	Thalamus_R	THA.R	0.047*	0.081	0.040*
Right middle temporal gyrus**	Temporal_Mid_R	MTG.R	0.116	0.021*	0.160
Right inferior temporal gyrus	Temporal_Inf_R	ITG.R	0.002*	0.021*	0.004*
Left cerebellum 10**	Cerebelum_10_L	CRBL10.L	0.013*	0.757	0.041*
Cerebellum vermis 9**	Vermis_9	Vermis9	0.047*	0.305	0.056

Note: Nodes that exhibited significant differences in at least one of the nodal centralities (*P<0.05, FWE uncorrected) were extracted. Based on these nodes, a key subset of connections was obtained by using a network-based statistics approach (**P<0.05, FWE corrected).

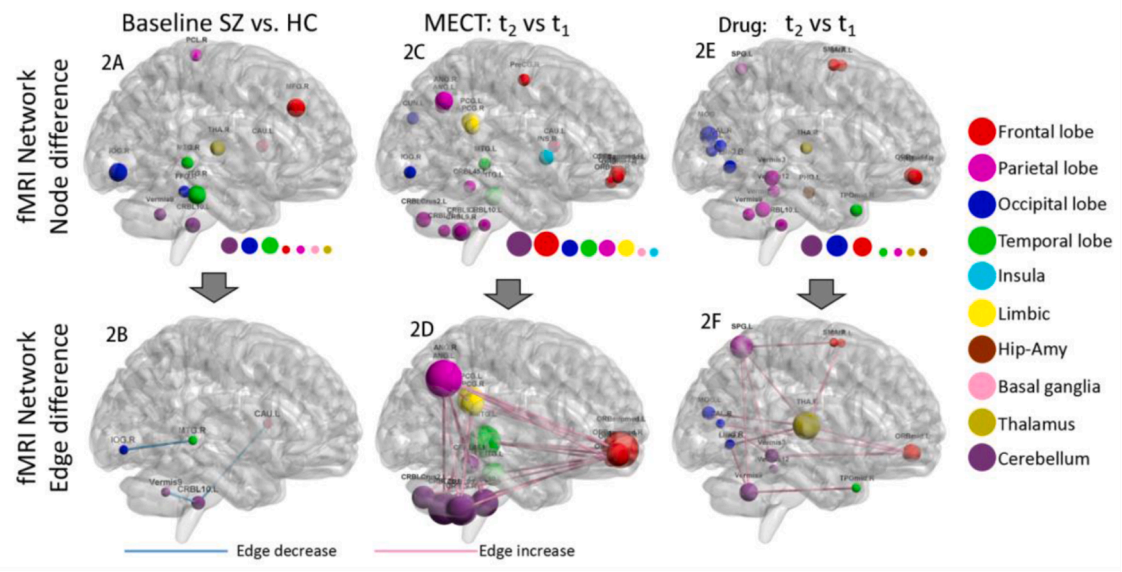

Fig. 2. Results of key sub-network analysis. The differences of node (A) and edge (B) of fMRI network between the baseline SZ group and HC group. The longitudinal changes of node (C) and edge (D) of fMRI network in the SZ patients following ECT. The longitudinal changes of node (E) and edge (F) of fMRI network in the SZ patients following antipsychotic treatment. SZ, Schizophrenia; HC, Healthy control; ECT, Modified Electroconvulsive therapy.

difference, Ganella's research used FMRIB Software Library to do the basic data preprocessing and applied different parameters from ours, which might contribute to the different results (Ganella et al., 2017). Different human races may have different brain structures in terms of brain size (Sivaswamy et al., 2019), shape, or volume (Tang et al., 2010, Jao et al., 2009). Jao's study also revealed that activation regions in response to specific tasks in the Chinese population differed from the activated regions in Caucasians (Jao et al., 2009). Different illness states of SZ imposed different impacts on the brain structures. Dietsche's study showed different extents of gray matter loss in preclinical subjects, first-episode SZ, and chronic SZ (Dietsche et al., 2017). Recent evidence proved that locations of aberrant FC are different for different illness states of SZ. For example, Li's study revealed abnormal FC in first-episode SZ was primarily detected in the frontal cortex. At the same time, aberrant FC in chronic SZ was primarily located in more diffused regions (Li et al., 2017).

In this study, the MSZ group showed reduced global efficiency after ECT. The DSZ group showed no changes after the antipsychotic treatments. However, the MSZ and DSZ groups do not differ in the PANSS total score and subscale score. We proposed that the changes of global efficiency in the MSZ group might be one potential mechanism of ECT effects, which was distinct from antipsychotics. In addition, there may be several reasons that can explain the insignificant result of the clinical outcome. In clinical practice, ECT is expected to associate with rapid and significant relieving of clinical symptoms, which can be reflected by a significant reduction of PANSS score. In our study, the clinical efficacy was reflected by the baseline and 4-week PANSS assessment. However, we only conducted the PANSS assessment at baseline and 4-week follow-up interview, in which we didn't know how symptoms changed between baseline and four weeks. It's feasible that the PANSS score may be reduced at a faster rate on week one or week two in the MSZ group. Unfortunately, we didn't have clinical data between baseline and four weeks. In addition, there may be long-term clinical efficacy of ECT, which can't be known in the present study. Meanwhile, the present study allocated the subjects to the MSZ or DSZ group based on patients' intentions and psychiatrists' advice in accordance with the regulation of IRB. Treatment-resistant patients are more willing to receive ECT treatment. The proportion of patients with a long duration of illness (over two years) in the MSZ group is marginally higher than the proportion in the DSZ group. Previous studies showed that a longer duration of illness predicted poorer treatment response in SZ patients (Altamura et al., 2015), which explained the equivalent treatment response between MSZ and DSZ groups since the MSZ group may be more treatment-resistant. Moreover, the number of previous failed antipsychotic trials in the MSZ group is marginally more than that in the DSZ group. In our present study, more patients from MSZ group (18 in 21)

Table 4
Brain regions that exhibited significant changes between pre-ECT and post-ECT in nodal efficiency, nodal betweenness and nodal degreex.

Regions	AAL Labels	Abbreviation	Permutation test p-values		
			Efficiency	Betweenness	Degree
Right precentral gyrus	Precentral_R	PreCG.R	0.035*	0.566	0.063
Right superior orbitofrontal cortex**	Frontal_Sup_Orb_R	ORBsup.R	0.520	0.048*	0.247
Left middle orbitofrontal cortex**	Frontal_Mid_Orb_L	ORBmid.L	0.054	0.768	0.011*
Right middle orbitofrontal cortex**	Frontal_Mid_Orb_R	ORBmid.R	0.092	0.433	0.042*
Left medial orbitofrontal cortex**	Frontal_Med_Orb_L	ORBsupmed.L	0.073	0.063	0.025*
Right medial orbitofrontal cortex**	Frontal_Med_Orb_R	ORBsupmed.R	0.092	0.715	0.025*
Right insula	Insula_R	INS.R	0.016*	0.357	0.021*
Left posterior cingulum**	Cingulum_Post_L	PCG.L	0.025*	0.030*	0.017*
Right posterior cingulum**	Cingulum_Post_R	PCG.R	0.019*	0.831	0.008*
Left cunues	Cuneus_L	CUN.L	0.715	0.049*	0.476
Right inferior occipital gyrus	Occipital_Inf_R	IOG.R	0.543	0.021*	0.590
Left angular gyrus**	Angular_L	ANG.L	0.035*	0.575	0.016*
Right angular gyrus**	Angular_R	ANG.R	0.013*	0.011*	0.008*
Left caudate	Caudate_L	CAU.L	0.394	0.040*	0.131
Left middle temporal gyrus**	Temporal_Mid_L	MTG.L	0.590	0.042*	0.414
Left inferior temporal gyrus**	Temporal_Inf_L	ITG.L	0.049*	0.030*	0.023*
Left cerebellum crus 2**	Cerebelum_Crus2_L	CRBLCrus2.L	0.079	0.022*	0.042*
Left cerebellum 4 and 5**	Cerebelum_4_5_L	CRBL45.L	0.768	0.049*	0.639
Left cerebellum 7b**	Cerebelum_7b_L	CRBL7b.L	0.073	0.099	0.035*
Left cerebellum 9**	Cerebelum_9_L	CRBL9.L	0.013*	0.017*	0.013*
Right cerebellum 9**	Cerebelum_9_R	CRBL9.R	0.073	0.433	0.049*
Left cerebellum 10**	Cerebelum_10_L	CRBL10.L	0.033*	0.073	0.133

Note: Nodes that exhibited significant differences in at least one of the nodal centralities (* $P<0.05$, FWE uncorrected) were extracted. Based on these nodes, a key subset of connections was obtained by using a network-based statistics approach (**$P<0.05$, FWE corrected).

Table 5
Brain regions that exhibited significant changes between pre-antipsychotics and post-antipsychotics in nodal efficiency, nodal betweenness, and nodal degree.

Regions	AAL Labels	Abbreviation	Permutation test p-values		
			Efficiency	Betweenness	Degree
Left middle orbitofrontal cortex**	Frontal_Mid_Orb_L	ORBmid.L	0.010*	0.170	0.006*
Right middle orbitofrontal cortex	Frontal_Mid_Orb_R	ORBmid.R	0.039*	0.998	0.023*
Left supplemental motor area**	Supp_Motor_Area_L	SMA.L	0.375	0.011*	0.394
Right supplemental motor are**	Supp_Motor_Area_R	SMA.R	0.357	0.044*	0.664
Left parahippocampal gyrus	ParaHippocampal_L	PHG.L	0.149	0.004*	0.131
Left calcarine	Calcarine_L	CAL.L	0.794	0.006*	0.958
Right calcarine**	Calcarine_R	CAL.R	0.566	0.021*	0.614
Left lingual gyrus**	Lingual_L	LING.L	0.455	0.025*	0.566
Right lingual gyrus**	Lingual_R	LING.R	0.181	0.030*	0.305
Left middle occipital gyrus**	Occipital_Mid_L	MOG.L	0.027*	<0.001*	0.042*
Left superior parietal lobe**	Parietal_Sup_L	SPG.L	0.114	0.030*	0.140
Right thalamus**	Thalamus_R	THA.R	0.289	0.028*	0.305
Right middle temporal pole**	Temporal_Pole_Mid_R	TPOmid.R	0.289	0.033*	0.205
Left cerebellum 10	Cerebelum_10_L	CRBL10.L	0.085	0.099	0.023*
Cerebellum vermis 1 and 2**	Vermis_1_2	Vermis12	0.106	0.184	0.040*
Cerebellum vermis 3**	Vermis_3	Vermis3	0.001*	0.062	0.002*
Cerebellum vermis 9**	Vermis_9	Vermis9	0.063	0.370	0.019*
Cerebellum vermis 10	Vermis_10	Vermis10	0.033*	0.389	0.031*

Note: Nodes that exhibited significant differences in at least one of the nodal centralities (* $P<0.05$, uncorrected) were extracted. Based on these nodes, a key subset of connections was obtained by using a network-based statistics approach (**$P<0.05$, FWE corrected).

were on over two kinds of antipsychotics, compared to the DSZ group (9 in 21). The evidence above gives hints that the MSZ group may be more treatment-resistant. In summary, compared to the DSZ group, the MSZ group had longer DUP, more failed trials of antipsychotics. They were also prescribed with more kinds of antipsychotics, all of which evidence suggested MSZs might be more treatment-resistant.

Recently, the cerebellum has been considered to play an essential role in the pathology of various kinds of mental illnesses. Accordingly, our study showed that the FC between the cerebellum and cerebrum was impaired in the SZ group at baseline. In line with our result, Brady and his colleagues also revealed that negative symptoms might be associated with the impairment of FC between the frontal cortex and cerebellum (Brady et al., 2019). The most significant finding of our study is that the aberrant FC between the cerebellum and cerebrum could be restored by an entire course of ECT. Specifically, our result showed that ECT could largely increase the FC between the cerebellum and cerebrum. Further, the change of FC between cerebellum and cerebrum was significantly associated with the reduction ratio of PANSS general psychopathology score but not associated with changes of PANSS positive or negative score. The PANSS general psychopathology involves items describing emotion, cognition, and behaviors. While cerebellum is involved in the process of emotion, cognition, and behaviors, which explains the association between the restoration of FC within the cerebellum-cerebrum neural loop and the improvement of PANSS general psychopathology.

The increased FC after ECT primarily involved the connections that link the DMN and the cerebellum, which indicated a weak connection between DMN and cerebellum before ECT in our sample. Different from our study, some studies reported increased functional connectivity between DMN and cerebellum in SZ (Wang et al., 2016, Guo et al., 2015, Bang et al., 2018). While these studies recruited first-episode psychosis or ultra-high risk for psychosis. Their cognition functions were not impaired, and they might exhibit normal cognitive functions with extra

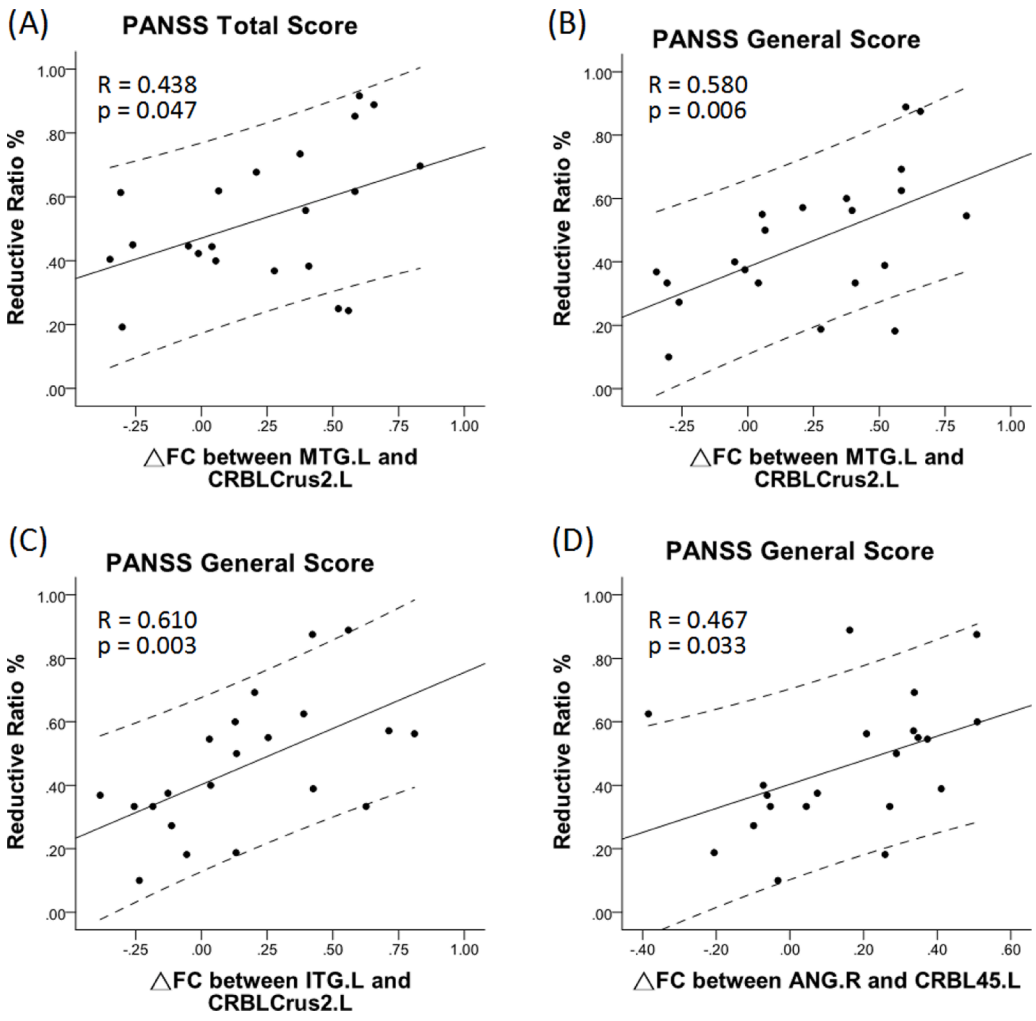

Fig. 3. The relationships between the key-network functional connectivity and clinical improvements in the MSZ group. (A) The △FC between the left middle temporal gyrus and left cerebellar crus2 region showed significant correlations with the reductive ratio of the PANSS total scores. (B) The △FC between the left middle temporal gyrus and left cerebellar crus2 region significantly correlated with the reductive ratio of the PANSS general psychopathology subscales. (C) The △FC between the left inferior temporal gyrus and left cerebellar crus2 region exhibited a significant correlation with the reductive ratio of the PANSS general psychopathology subscales. (D) The △FC between the right angular and left cerebellar 45 regions were significantly correlated with the reductive ratio of the PANSS general psychopathology subscales.

effort (Frydecka et al., 2016). Subjects in the MSZ group were treatment-resistant and had a longer disease duration, which would impose negative influences on the functions of DMN. In line with this hypothesis, our previous study showed that ECT could enhance the function of the DMN in SZ (Huang et al., 2018), who had a low DMN function at baseline (Guo et al., 2017). Furthermore, one prior study showed the FC connecting the cerebellum with DMN was involved in the process of attention switching. Impaired attention was implicated in treatment-resistant SZ (Anderson et al., 2015, Young and Wimmer, 2017).

As for the DSZ group, we found that a key sub-network was altered after a 4-week treatment with antipsychotics. The sub-network was primarily the thalamus, cerebellum, and cerebral cortices. Although the cerebellum was also involved in antipsychotic efficacy on SZ, the nodes and edges engaged in this process were quite limited compared to the MSZ group. Since abnormal sensory perception is one critical clinical feature of schizophrenia, we proposed that the thalamus, relaying sensory information to the cerebrum, might be impaired in schizophrenia. Several previous studies have confirmed deficits in thalamus structure and function in SZ (Huang et al., 2015, Hua et al., 2019, Hamoda et al., 2019). Hua et al. identified decreased FC between subregions of the thalamus and prefrontal cortex, with the technique of 7T fMRI (Hua et al., 2019). In the present study, both groups showed altered FC at follow-up. However, only the MSZ group yielded the association between FC changes and the reductive ratio of PANSS total and PANSS general psychopathology. We proposed that antipsychotics might improve clinical symptoms indirectly through the identified neural network in the DSZ group. Some medium mechanisms might exist. At last, ECT possibly shows its antipsychotic effects by acting on the cerebrum-cerebellum loop.

5. Limitation

There are several limitations of our study. First, the allocation of SZ patients to the MSZ or DSZ group is not randomized, which led to some differences in the clinical background between the two groups, such as duration of illness. The non-random strategy would inevitably introduce selection bias, which might impose influences on the results. Under psychiatrists' advice, MSZ groups might involve severer or treatment-resistant patients. Meanwhile, the DSZ group possibly involves more patients with milder symptoms. In our future study, we may consider only involving patients willing to receive ECT and conduct a randomized trial to further investigate ECT neural mechanism. Second, the study duration is too short to see the long-term effects of ECT on both the clinical improvement and large-scale cerebral network. In our future study, we will try to reduce the confounders and re-schedule the follow-up plan covering shorter time (week 1, week2, week 3) and longer time (6 months, year 1, year 2) to investigate the possible clinical outcome in association to ECT. Third, different kinds or doses of antipsychotics were prescribed to patients, which definitely would introduce confounding factors, however as regulated by our protocol, antipsychotic doses were fixed for each patient during the whole study period, which introduced less bias to our results. And the chlorpromazine equivalence doses for MSZ and DSZ group wasn't significantly different, which would make

our results more reliable. Furthermore, we will recruit an additional depression group to explore whether the antipsychotic effect of ECT is distinct from its anti-depression effect. Fifth, the second MRI was scanned 24–48 h after the last ECT. The scanning interval may be too short, considering that neuropsychological deficits last almost 72 hours (Calev et al., 1995) and the water content of the brain might still be increased by then (Mander et al., 1987). We will increase the scan interval in our future research. In addition, we didn't collect cognition data before and after ECT. The ECT-induced cognition impairment may interfere with the clinical assessment at follow-up. Finally, our research was observational, and results should be interpreted cautiously.

6. Conclusion

Schizophrenia is an illness of the whole brain, including the cerebellum. The cerebral-cerebellum loop is possibly involved in the antipsychotic mechanisms of ECT.

Fundings

This work was supported by grants from National Natural Science Foundation of China grants (82151314, 81971251, 81671329, and 81871050, 82171497, 82101582, 82001406); Clinical Research Center at Shanghai Mental Health Center grants (CRC2018ZD01, CRC2018ZD04, and CRC2018YB01, CRC2019ZD02, 2020-FX-02); Clinical Research Center at Shanghai Jiaotong University School of Medicine (DLY201817, 20190102); Shanghai Science and Technology Committee Foundations (19411950800, 16ZR1430500, 19411969100, 19410710800, 21ZR1481500, 20ZR1448600, 21S31903100, 19ZR14451); the Science and Technology Commission of Shanghai Municipality (19411969400); Shanghai Clinical Research Center for Mental Health (19MC1911100); Project of the Key Discipline Construction, Shanghai 3-Year Public Health Action Plan (GWV-10.1-XK18); Shanghai Municipal Science and Technology Major Project (No.2018SHZDZX01, 2018SHZDZX05) and ZJLab; Qihang Foundation of Shanghai Mental Health Center (2019-QH-01), Fund for Talents by Shanghai Mental Health Center [grant number 2018-FX-04], China Postdoctoral Science Foundation (BX2021078) and Excellent Talents Training Project of Shanghai Municipal Commission of Health (GWV-10.2-YQ44).

Declaration of Competing Interest

None.

Acknowledgments

We thank all the participants who attended the study.

References

Meltzer, H.Y., 1997. Treatment-resistant schizophrenia–the role of clozapine. Curr. Med. Res. Opin. 14 (1), 1–20.
Elkis, H., 2007. Treatment-resistant schizophrenia. Psychiatr. Clin. North Am. 30 (3), 511–533.
Howes, O.D., et al., 2017. Treatment-Resistant Schizophrenia: Treatment Response and Resistance in Psychosis (TRRIP) Working Group Consensus Guidelines on Diagnosis and Terminology. Am. J. Psychiatry 174 (3), 216–229.
Tharyan, P. and C.E.J.C.D.o.S.R. Adams, Electroconvulsive therapy for schizophrenia. 2005(2).
Lally, J., et al., 2016. Augmentation of clozapine with electroconvulsive therapy in treatment resistant schizophrenia: A systematic review and meta-analysis. Schizophr. Res. 171 (1–3), 215–224.
Jiang, J., Wang, J., Li, C., 2017. Potential Mechanisms Underlying the Therapeutic Effects of Electroconvulsive Therapy. Neurosci. Bull. 33 (3), 339–347.
Flace, P., et al., 2018. The Neglected Cerebello-Limbic Pathways and Neuropsychological Features of the Cerebellum in Emotion. Cerebellum 17 (2), 243–246.
Sokolov, A.A., Miall, R.C., Ivry, R.B., 2017. The Cerebellum: Adaptive Prediction for Movement and Cognition. Trends Cogn. Sci. 21 (5), 313–332.
Wang, D., et al., 2019. Topological Disruption of Structural Brain Networks in Patients With Cognitive Impairment Following Cerebellar Infarction. Front. Neurol. 10, 759.
Castellazzi, G., et al., 2018. Prominent Changes in Cerebro-Cerebellar Functional Connectivity During Continuous Cognitive Processing. Front. Cell Neurosci. 12, 331.
Carta, I., et al., 2019. Cerebellar modulation of the reward circuitry and social behavior. Science (6424), 363.
Villanueva, R., 2012. The cerebellum and neuropsychiatric disorders. Psychiatry Res. 198 (3), 527–532.
Andreasen, N.C., Pierson, R., 2008. The role of the cerebellum in schizophrenia. Biol. Psychiatry 64 (2), 81–88.
Hirjak, D., et al., 2015. Neurological soft signs in recent-onset schizophrenia: Focus on the cerebellum. Prog. Neuropsychopharmacol. Biol. Psychiatry 60, 18–25.
Sathyanesan, A., et al., 2019. Emerging connections between cerebellar development, behaviour and complex brain disorders. Nat. Rev. Neurosci. 20 (5), 298–313.
Chen, G., et al., 2019. Abnormal cerebellum-DMN regions connectivity in unmedicated bipolar II disorder. J. Affect. Disord. 243, 441–447.
Surguladze, S.A., et al., 2011. Emotion processing in schizophrenia: fMRI study of patients treated with risperidone long-acting injections or conventional depot medication. J. Psychopharmacol. 25 (6), 722–733.
Brady Jr., R.O., et al., 2019. Cerebellar-Prefrontal Network Connectivity and Negative Symptoms in Schizophrenia. Am. J. Psychiatry 176 (7), 512–520.
Zhuo, C., et al., 2018. Altered resting-state functional connectivity of the cerebellum in schizophrenia. Brain Imaging Behav. 12 (2), 383–389.
Guo, W., et al., 2018. Treatment effects of olanzapine on homotopic connectivity in drug-free schizophrenia at rest. World J. Biol. Psychiatry 19 (sup3), S106–s114.
Pawelczyk, T., et al., 2014. Effectiveness and clinical predictors of response to combined ECT and antipsychotic therapy in patients with treatment-resistant schizophrenia and dominant negative symptoms. Psychiatry Res. 220 (1–2), 175–180.
Usta Saglam, N.G., et al., 2020. ECT augmentation of antipsychotics in severely ill schizophrenia: a naturalistic, observational study. Int. J. Psychiatry Clin. Pract. 24 (4), 392–397.
Thomann, P.A., et al., 2017. Neuromodulation in response to electroconvulsive therapy in schizophrenia and major depression. Brain Stimul. 10 (3), 637–644.
Takano, H., et al., 2011. Differences in cerebral blood flow between missed and generalized seizures with electroconvulsive therapy: A positron emission tomographic study. Epilep. Res. 97 (1), 225–228.
Wei, Q., et al., 2020. Enhanced cerebro-cerebellar functional connectivity reverses cognitive impairment following electroconvulsive therapy in major depressive disorder. Brain Imaging Behav.
Andreasen, N.C., et al., 2010. Antipsychotic dose equivalents and dose-years: a standardized method for comparing exposure to different drugs. Biol. Psychiatry 67 (3), 255–262.
Kellner, C.H., et al., 2010a. Bifrontal, bitemporal and right unilateral electrode placement in ECT: randomised trial. Br. J. Psychiatry 196 (3), 226–234.
Kellner, C.H., Tobias, K.G., Wiegand, J., 2010b. Electrode placement in electroconvulsive therapy (ECT): A review of the literature. J. ECT 26 (3), 175–180.
Peterchev, A.V., et al., 2010. Electroconvulsive therapy stimulus parameters: rethinking dosage. J. ECT 26 (3), 159–174.
Jiang, Y., et al., 2019. Insular changes induced by electroconvulsive therapy response to symptom improvements in schizophrenia. Prog. Neuropsychopharmacol. Biol. Psychiatry 89, 254–262.
Huang, H., et al., 2018. Increased resting-state global functional connectivity density of default mode network in schizophrenia subjects treated with electroconvulsive therapy. Schizophr. Res. 197, 192–199.
Wang, J., et al., 2015. GRETNA: a graph theoretical network analysis toolbox for imaging connectomics. Front. Hum. Neurosci. 9, 386.
Guo, X., et al., 2019. Enhancement of indirect functional connections with shortest path length in the adult autistic brain. Hum. Brain Mapp. 40 (18), 5354–5369.
Jiang, Y., et al., 2020. Characteristics of disrupted topological organization in white matter functional connectome in schizophrenia. Psychol. Med. 1–11.
Tzourio-Mazoyer, N., et al., 2002. Automated anatomical labeling of activations in SPM using a macroscopic anatomical parcellation of the MNI MRI single-subject brain. Neuroimage 15 (1), 273–289.
Yu, M., et al., 2017. Convergence and Divergence of Brain Network Dysfunction in Deficit and Non-deficit Schizophrenia. Schizophr. Bull. 43 (6), 1315–1328.
Adhikari, A., et al., 2015. Basomedial amygdala mediates top-down control of anxiety and fear. Nature 527 (7577), 179–185.
Zhang, J., et al., 2011. Disrupted brain connectivity networks in drug-naive, first-episode major depressive disorder. Biol. Psychiatry 70 (4), 334–342.
He, Y., et al., 2009. Impaired small-world efficiency in structural cortical networks in multiple sclerosis associated with white matter lesion load. Brain 132 (Pt 12), 3366–3379.
Zalesky, A., Fornito, A., Bullmore, E.T., 2010. Network-based statistic: identifying differences in brain networks. Neuroimage 53 (4), 1197–1207.
Groppe, D.M., Urbach, T.P., Kutas, M., 2011. Mass univariate analysis of event-related brain potentials/fields I: a critical tutorial review. Psychophysiology 48 (12), 1711–1725.
Alexander-Bloch, A.F., et al., 2010. Disrupted modularity and local connectivity of brain functional networks in childhood-onset schizophrenia. Front. Syst. Neurosci. 4, 147.
Lynall, M.E., et al., 2010. Functional connectivity and brain networks in schizophrenia. J. Neurosci. 30 (28), 9477–9487.
Micheloyannis, S., 2012. Graph-based network analysis in schizophrenia. World J. Psychiatry 2 (1), 1–12.
Moritz, S., Woodward, T.S., 2005. Jumping to conclusions in delusional and non-delusional schizophrenic patients. Br. J. Clin. Psychol. 44 (Pt 2), 193–207.

Ganella, E.P., et al., 2017. Functional brain networks in treatment-resistant schizophrenia. Schizophr. Res. 184, 73–81.
Sun, Y., et al., 2019. Dynamic Reorganization of Functional Connectivity Reveals Abnormal Temporal Efficiency in Schizophrenia. Schizophr. Bull. 45 (3), 659–669.
Su, T.W., et al., 2015. Schizophrenia symptoms and brain network efficiency: A resting-state fMRI study. Psychiatry Res. 234 (2), 208–218.
Sivaswamy, J., et al., 2019. Construction of Indian human brain atlas. Neurol. India 67 (1), 229–234.
Tang, Y., et al., 2010. The construction of a Chinese MRI brain atlas: a morphometric comparison study between Chinese and Caucasian cohorts. Neuroimage 51 (1), 33–41.
Jao, T., et al., 2009. Development of NTU standard Chinese Brain Template: morphologic and functional comparison with MNI template using magnetic resonance imaging. Annu. Int. Conf. IEEE Eng. Med. Biol. Soc. 2009, 4779–4782.
Dietsche, B., Kircher, T., Falkenberg, I., 2017. Structural brain changes in schizophrenia at different stages of the illness: A selective review of longitudinal magnetic resonance imaging studies. Aust. N. Z. J. Psychiatry 51 (5), 500–508.
Li, T., et al., 2017. Brain-Wide Analysis of Functional Connectivity in First-Episode and Chronic Stages of Schizophrenia. Schizophr. Bull. 43 (2), 436–448.
Altamura, A.C., Serati, M., Buoli, M., 2015. Is duration of illness really influencing outcome in major psychoses? Nord. J. Psychiatry 69 (6), 403–417.
Wang, H., et al., 2016. Patients with first-episode, drug-naive schizophrenia and subjects at ultra-high risk of psychosis shared increased cerebellar-default mode network connectivity at rest. Sci. Rep. 6, 26124.
Guo, W., et al., 2015. Increased Cerebellar Functional Connectivity With the Default-Mode Network in Unaffected Siblings of Schizophrenia Patients at Rest. Schizophr. Bull. 41 (6), 1317–1325.
Bang, M., et al., 2018. Aberrant cerebro-cerebellar functional connectivity and minimal self-disturbance in individuals at ultra-high risk for psychosis and with first-episode schizophrenia. Schizophr. Res. 202, 138–140.
Frydecka, D., et al., 2016. Profiling cognitive impairment in treatment-resistant schizophrenia patients. Psychiatry Res. 235, 133–138.
Guo, W., et al., 2017. Olanzapine modulation of long- and short-range functional connectivity in the resting brain in a sample of patients with schizophrenia. Eur. Neuropsychopharmacol. 27 (1), 48–58.
Anderson, V.M., et al., 2015. Does cognitive impairment in treatment-resistant and ultra-treatment-resistant schizophrenia differ from that in treatment responders? Psychiatry Res. 230 (3), 811–818.
Young, A., Wimmer, R.D., 2017. Implications for the thalamic reticular nucleus in impaired attention and sleep in schizophrenia. Schizophr. Res. 180, 44–47.
Huang, P., et al., 2015. Decreased bilateral thalamic gray matter volume in first-episode schizophrenia with prominent hallucinatory symptoms: A volumetric MRI study. Sci. Rep. 5, 14505.
Hua, J., et al., 2019. Altered functional connectivity between sub-regions in the thalamus and cortex in schizophrenia patients measured by resting state BOLD fMRI at 7T. Schizophr. Res. 206, 370–377.
Hamoda, H.M., et al., 2019. Abnormalities in thalamo-cortical connections in patients with first-episode schizophrenia: a two-tensor tractography study. Brain Imaging Behav. 13 (2), 472–481.
Calev, A., et al., 1995. ECT and non-memory cognition: a review. Br. J. Clin. Psychol. 34 (4), 505–515.
Mander, A.J., et al., 1987. Cerebral and brain stem changes after ECT revealed by nuclear magnetic resonance imaging. Br. J. Psychiatry 151 (1), 69–71.